Characteristics of Microtremors On Ground with Discontinuous Underground Structure

AUTHOR(S):

IRIKURA, Kojiro; KAWANAKA, Taku

CITATION:

IRIKURA, Kojiro ...[et al]. Characteristics of Microtremors On Ground with Discontinuous Underground Structure. Bulletin of the Disaster Prevention Research Institute 1980, 30(3): 81-96

ISSUE DATE:

1980-11

URL:

http://hdl.handle.net/2433/124892

Characteristics of Microtremors On Ground with Discontinuous Underground Structure

By Kojiro IRIKURA and Taku KAWANAKA*

(Manuscript received November 10, 1980)

Abstract

The characteristics of microtremors are examined, which were observed in an area having underground structures with vertical discontinuities. The work in now going on is made near the eastern edge of the southern part of Kyoto basin. The spatial correlation characteristics of microtremors are significantly affected by the vertical discontinuities of surface-soil layers. The phase velocities of vertical components show the dispersive nature of Rayleigh waves. The microtremors in this area tend to propagate from plain side to hill side, i.e. thick layer side to thin layer one. The tremors of wave length shorter than the thickness of the thin layer seem to be converted to a new mode soon after coming across a vertical discontinuity, but those of sufficiently longer wave lengths seem to sustain the old mode for a longer distance. The lateral variation of the amplitude of microtremors is explained in terms of the transmission and reflection of surface waves at a vertical discontinuity.

1. Introduction

It is often reported that earthquake damage tends to concentrate in a narrow area where the local geological configurations have steeply lateral variations. This shows that it is necessary for an engineering-seismological study to estimate amplification effects of earthquake motions not only by the vertical interferences within flat surface-layers but also by lateral ones associated with horizontal geological-irregularities. For example, intense damage at the Scopie Earthquake in 1963 is recorded along a belt which is defined by an abrupt change of the thickness of the alluvium (Poceski, 1969)[1]. Also, the damage region at the northern Yamanashi Earthquake in 1976 are situated remarkably along the Tsurukawa fault belt (Murai, et al., 1977)[2]. In the 1976 Friuri Earthquake (Italy), most of the severely damaged houses are distributed either on the slopes of mountains or on the alluvial soil layers adjacent to the slopes (Sasaki, et al., 1978)[3].

Therefore, it is necessary in presuming risk regions during earthquakes to find out the areas where underground structures have abrupt variations. The purpose of this study is to present a method for detecting the areas underlain by lateral irregularities by the use of the readily observable data of microtremors and to estimate the seismic responses at such areas.

* Present address: Japan Petroleum Exploration Company Limited.

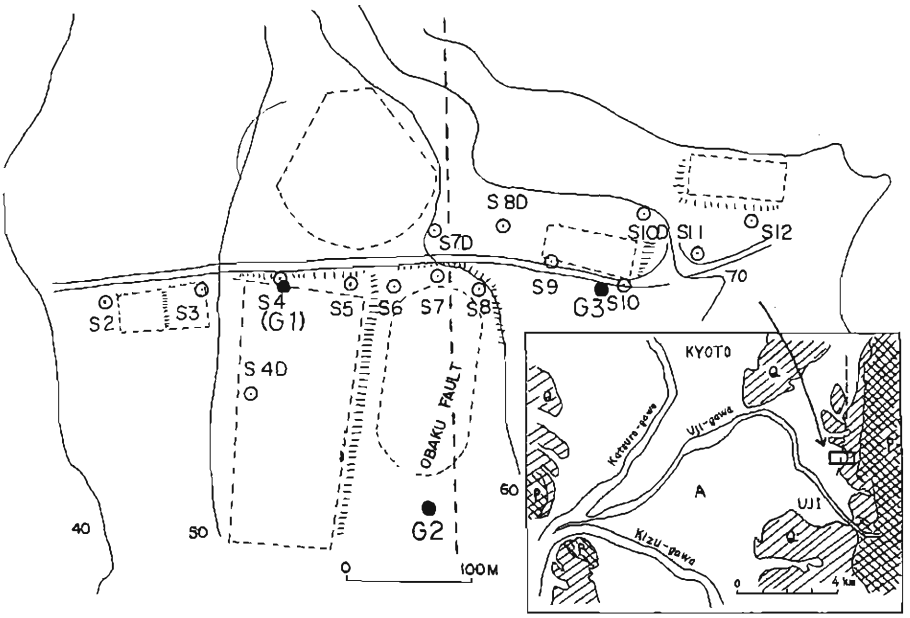

Fig. 1. Topographical map in this study area and locations of observation points.
P: Paleozoic rocks, Q: Terrace deposits of deluvium, A: Alluvial deposits.

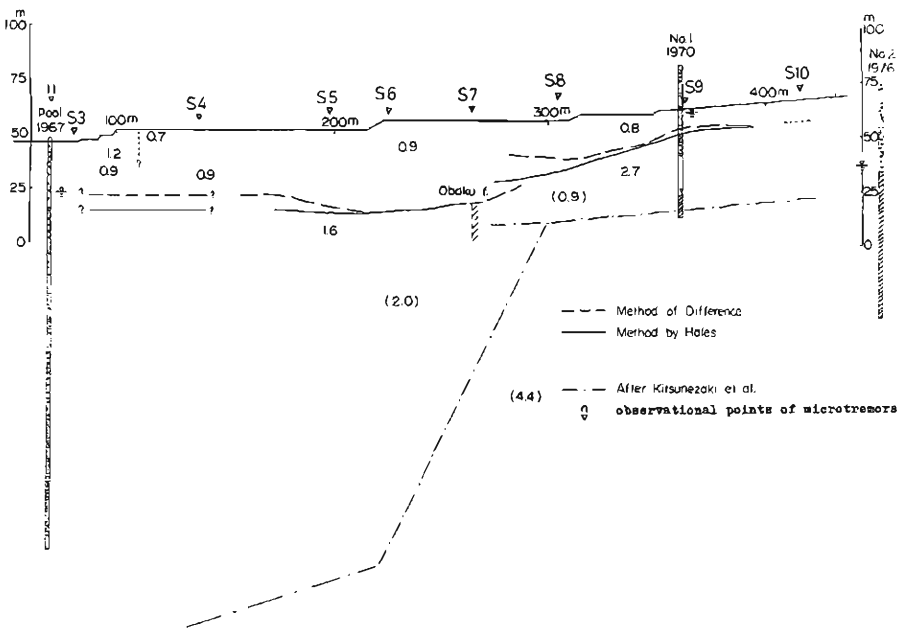

Fig. 2. Underground structures along east-west line determined by Kitsunezaki et al[4]., and Kobayashi et al[5].

The area near the eastern edge of the southern part of Kyoto basin provides favorable conditions to examine this problem. Refraction surveys in this area show that the underground structure from east to west has a vertical discontinuity which is inferred to be located on an extension of the Obaku fault. We observed the spatial distributions of the amplitudes and the phase velocities of microtremors over this area to study how the characteristics are affected by the lateral variations of the underground structures. The spatial variations of the power spectra are examined in terms of the transmission and reflection of surface waves at a vertical discontinuity.

Only predominant frequencies of microtremors have been used to estimate the seismic characteristics of grounds in most cases, by means of the method developed by Kanai, et al.[7]. From a new point of view, the usefullness and the limit of applicability of microtremor data are discussed in this paper for the purpose of predicting where the seismic motions may be severe during earthquakes.

2. Geological Features of Observation Sites and Method of Observation

The study area is located at the eastern side of the southern part of Kyoto basin, as shown in the right-lower insert of Fig. 1. There extends a plain to the west of this area and come near hills to the east. It is reported that the plain part is formed of alluvium and diluvium and the hills part is composed of paleozoic strata (Kitsunezaki, et al., 1971)[4].

The underground structure in this area was first estimated by Kitsunezaki et al. in 1971. They carried out seismic refraction exploration by means of five explosion sources on a long measuring line of about 12 km, ranging from the middle part of the basin to the eastern edge. In that survey, they found out that the thicknesses of soil deposits changed rapidly on the eastern side of the basin and the discontinuity was inferred to be located on an extension of the Obaku fault. In order to determine the underground structures in detail near the postulated fault, Kobayashi, et al. (1980)[5] carried out refraction exploration on a short measuring line of about 600 m across the discontinuity by a procedure of a stacking method employing a land-type air gun.

The east-to-west underground profile is shown in Fig. 2, obtained by the above two explorations. The soil deposits are formed of alluvium of P wave velocity less than 1 km/sec and thickness of 10 to 20 m in the first layer, and diluvium in the second layer, which is thick on the west side of the discontinuity and thin on the east side.

The observation points used for microtremors are shown by the open circles such as S2, S3 and so on, in Fig. 1. The observations of three components, V, NS and EW, were made simultaneously at three points for each observation. The observational points are moved from place to place to examine the spatial variations of the amplitudes and phases of the microtremors over this study area. The observation time is between 11 p.m. and 4 a.m., during which time the amplitude

levels of microtremors become the lowest during any day. The prominent noise sources such as main roads, railways and factories are distributed, mostly to the west, by more than several hundreds meters.

The sensing instruments are 3-components sets of short-period velocity seismometers having a natural period of 1.0 sec, damping ratio of 0.64 to critical and sensitivity of 3 volt/kine. The output signals from each seismometer are recorded in analog form on magnetic tapes, after being amplified 1000 to 3000 times through amplifieres of DC types. The data on the magnetic tape are converted to digital form at a sampling interval of 0.01 sec for processing by computer.

3. Power Spectra of Microtremors

The influence of a vertical discontinuity of the underground structure to the characteristics of microtremors is examined, by comparing the power spectra obtained simultaneously at some points on both sides of the postulated fault. For the computation of power spectra, the length of the analysis is 40.84 sec and the Hamming window is employed for smoothing spectra.

The power spectra of the vertical components are shown in the left figures of Fig. 3a, simultaneously observed at the three points, S4, S8 and S12. S4 is on the west side of the discontinuity and underlain by thicker soil layers, S12 is on the east side and underlain by thinner soil layers, and S8 is over near the discontinuity. Solid, dashed and chained curves show the power spectra observed for the intervals of about 2 hours during a night to examine the time-stationary characteristics of microtremors. The right figures show the power spectral ratios which are the ratios of the square roots of the power spectra between the two points. S4/S12 and S4/S8 mean the power spectral ratios between the point S4 and S12 and those between the point S4 and S8, respectively. The same expression is used after this. In the left figure of Fig. 3a, each power spectrum at each point fluctuates each time to some extent, but the power spectral ratios between the two points do not fluctuate much with every observation. The microtremors at S4 had relatively intense powers in comparison with those at S8 and S12. The ratios for S4/S12 observations have a significant peak around 2 Hz and are about 10 at the peak frequency. On the other hand, the ratios, S8/S12 show comparatively smoothed curves, having not such significant peaks.

The power spectra of the horizontal NS and EW components at S4, S8 and S12 are shown in the left figures of Fig. 3b and Fig. 3c, and the ratios between the two points, S4/S8 and S8/S12 are shown in the right figures, respectively. Similar to the cases of vertical components, S4 has intense power spectra in comparison with S8 and S12. The ratios for S4/S12 observations have a peak around 1.2 Hz and are about 5 at the peak frequency in both cases of NS and EW components. The ratios for S8/S12 observations are relatively smooth in comparison with the those for S4/S12. The remarkable differences between the ratios of S4 to S12 and those of S8 to S12 are considered to be influenced by the horizontal irregularity of the

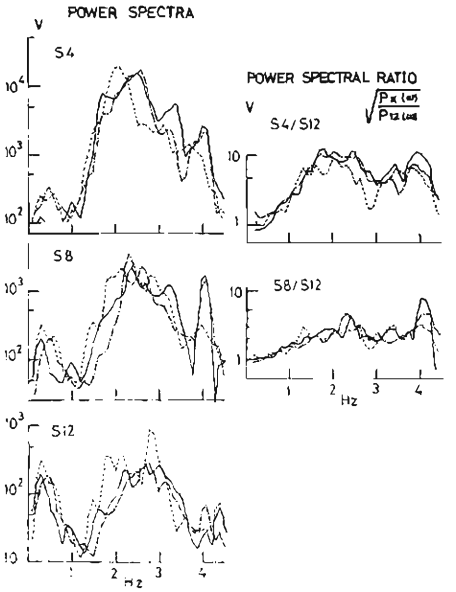

Fig. 3a. Power spectra of microtremors observed simultaneously at three points of S4, S8 and S12 and ratios of square roots of power spectra of S4 and S8 to S12. Case of vertical component.

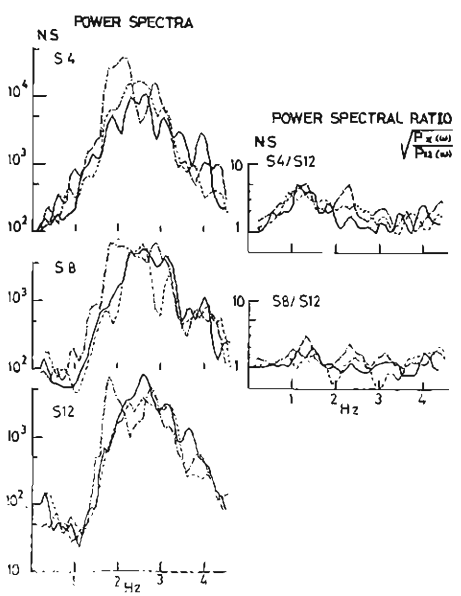

Fig. 3b. Case of horizontal NS components.

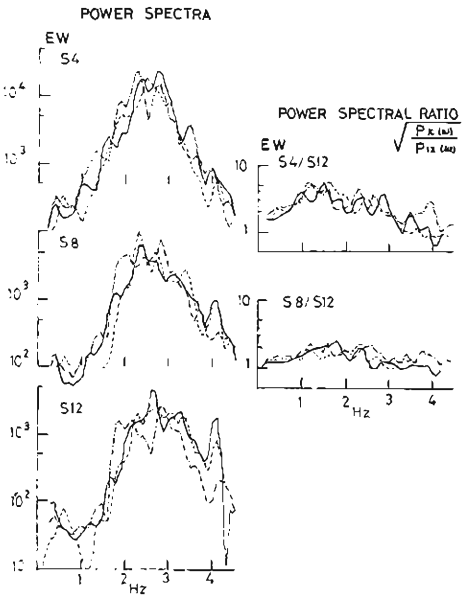

Fig. 3c. Case of horizontal EW components.

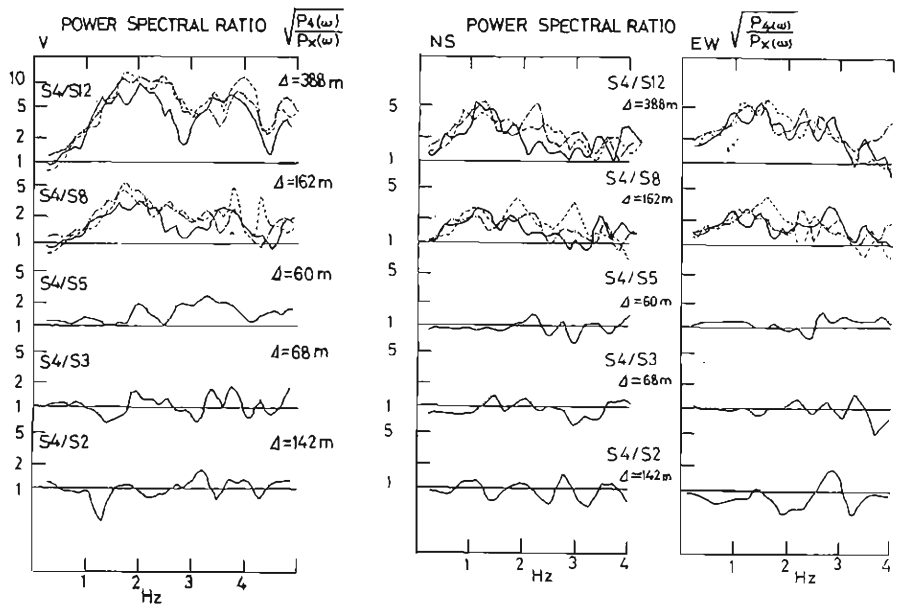

Fig. 4. Ratios of square roots of power spectra at S4 to those at S2, S3, S5, S8 and S12.

underground structure existing between the points S4 and S8.

In Fig. 4, the power-spectral ratios of S4 to S2, S3, S5, S8 and S12 are arranged to show where the power spectra of microtremors change most remarkably. The left figure shows the power spectral ratios for the vertical components and the right two figures show those of horizontal NS and EW components, respectively. These curves show some apparent tendencies. The larger the specified number of the observational point becomes (that is, as it moves to east), the smaller the amplitude of the power spectrum becomes. The ratios for S4/S2, S4/S3 and S4/S5 are nearly equal to unity in both the vertical and the horizontal components in the frequency ranges of 0.3 to 5.0 Hz, though they fluctuate at the higher frequencies. On the other hand, the ratios for S4/S8 and S4/S12 are significantly larger than those for S4/S2, S4/S3 and S4/S5 and have a common peak around 1.8 Hz in the case of the vertical components and around 1.2 Hz in the case of NS and EW components.

In order to make more detailed discussions, the power spectral ratios are shown in Fig. 5, between the observational points near the very top of the postulated fault. The left figures show the ratios between the points S7D and S8, and between the points S7D and S8D. As shown in Fig. 1, the fault is inferred to exist between these 2 points. The right figures show the ratios between the points S8 and S9, and between the points S8D and S9. The fault does not seem to exist between these points. The ratios in the right figures are nearly equal to unity in the frequency range up to 5 Hz, and on the other hand those in the left figures are considerably less than unity in the frequency range larger than 1 Hz. The power-spectral ratios

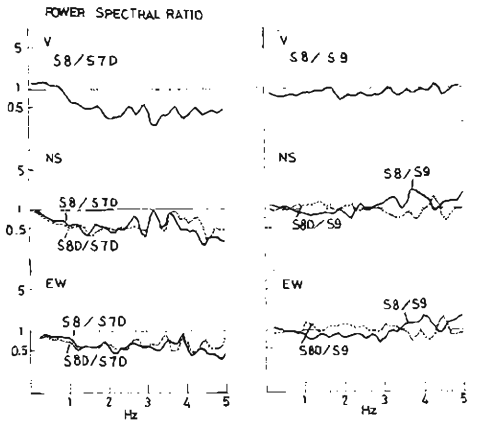

Fig. 5. Ratios of square roots of power spectra between the two points near the very top of the postulated fault. The fault is inferred to exist between the points S8 and S7D and between the points S8D and S7D, and not to exist between the points S8 and S9.

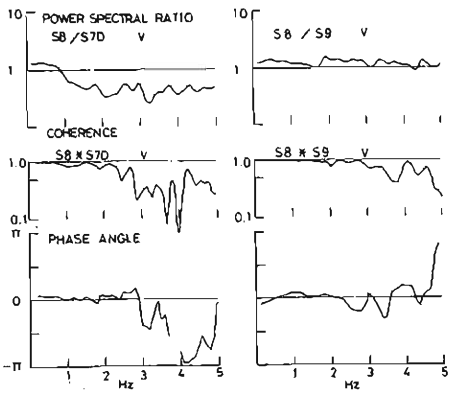

Fig. 6. Ratios of square roots of power spectra, coherences and coherent angles. The fault is inferred to exist between the points S8 and S7D and not to exist between the points S8 and S9.

between the two points are found to change clearly, depending on whether the fault exists between the two points or not.

The power spectral ratios, the coherences and coherent angles of the vertical components between S8 and S9 and between S8 and S7D are shown in Fig. 6. The coherences between S8 and S7D decrease steeply at the frequencies higher than 2.5 Hz and the phase angles change largely at the same frequencies. The frequency range in which coherences are uniform extends to higher frequency in comparison with that in which the power spectral ratios are close to unity. These phenomena are considered to be caused by the nature of progressive surface waves over the vertical discontinuity; the progressive surface waves continue for a short while as the waves of old type, even after they have run into a new structure (Alsop, et al., 1974)[6]. On the other hand, the coherence and the coherent angle between S8 and S9 change slowly in the frequency range close to 5 Hz. This also is considered to reflect the fact that a vertical discontinuity does not exist between these two points.

Till quite recently, as a method of estimating ground characteristics during earthquakes, only predominant frequencies of microtremors by observing microtremors individually at a lot of points have been used. However, a correlation between the predominant frequencies and the thicknesses of the surface layers does not always exist. For example, the power spectra of the horizontal components shown in Fig. 3b and 3c have a common peak around 2.5 Hz at all points, which are set across a vertical discontinuity as above mentioned. On the other hand, the spectral ratios between the two points vary spatially, depending on whether the reference points exist across the discontinuity.

4. Phase Velocities of Microtremors

The relation between the propagation characteristics of microtremors and vertical discontinuities of underground structures is examined in this section. The observations were made to obtain the phase velocities of microtremors on the both sides of the fault, side A and side B, as shown in Fig. 7. The phase velocities on side A and side B were estimated, employing the appropriate combinations of 3 points forming a tripartite array among 5 points, (A2, A3, A4, A4D-1 and A4D-2) and (B8, B9, B10, B8D-1 and B8D-2), respectively. The phase differences of vertical components between the two points were determined as a function of frequency using the phase angles of the crosspower spectra. The interval for the analysis was 10.24 sec and the maximum of the

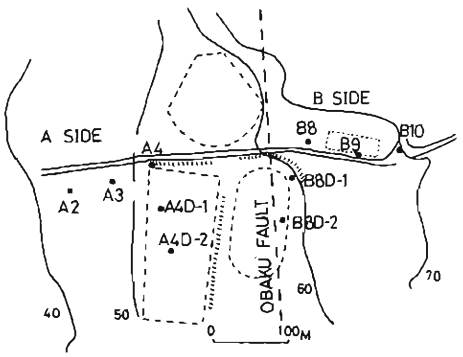

Fig. 7. Locations of observation points for determination of phase velocities of microtremors.

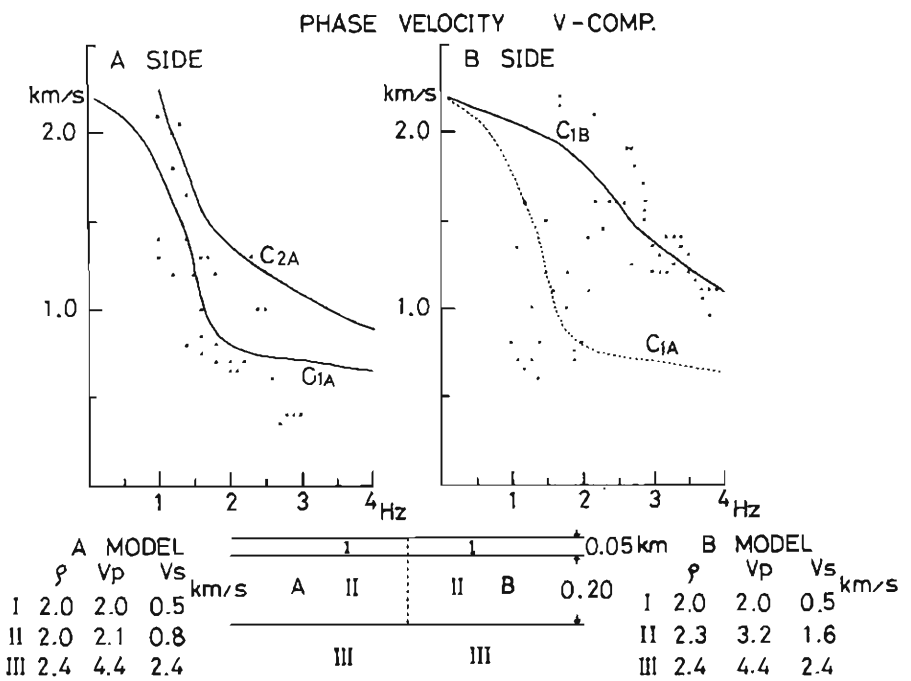

Fig. 8. Phase velocities observed and theoretical dispersion curves of Rayleigh waves, assuming to be flat layers. C_{1A} and C_{2A}; the fundamental and the first higher mode of model A. C_{1B} the fundamental mode of model B.

lag time of the correlation was taken to be 2.56 sec. The phase velocities obtained are plotted in Fig. 8. The left and right figures show the phase velocities as a function of frequency on side A and side B, respectively.

The phase velocities on side A are clearly dispersive, being slower as the frequency becomes higher. The directions of propagation are mostly eastward, i.e. from side A to side B. This is consistent with the fact that noise sources exist mostly to the west, i.e. the plain side. On the other hand, the phase velocities on side B appear to be divided into two parts. One is the phase velocities in the frequency range higher than 2 Hz, appearing clearly dispersive. The other is those in the range lower than 2 Hz, being largely scattered. The theoretical phase-velocity curves of Rayleigh waves are calculated by assuming such flat layers as shown by the bottom figure in Fig. 8. C_{1A}, C_{2A} and C_{1B} show the fundamental mode on side A, the first higher mode on side A and the fundamental mode on side B. The phase velocities observed on side A seem to be in good agreement with the dispersion curves of the fundamental mode, as shown in the left figure of Fig. 8. On the other hand, the phase velocities observed on side B do not correspond simply to the dispersion curves on side B. Those in the frequency range higher than 2 Hz may be regarded as roughly consistent with the dispersion curves of the fundamental mode on side B. However, those in the range lower than 2 Hz would be better regarded as the fundamental mode on side A rather than the mode on side B. It is qualitatively considered that the tremors of wave lengths sufficiently longer than the layer thickness of side B continue the old mode for a short distance on side B, while those of shorter wave lengths are converted to a new mode soon after running into side B. This is consistent with the results where the coherence between the two points across the vertical discontinuity remains close to unity up to higher frequencies in comparison with the frequencies in which the power spectral ratios decrease steeply as shown by Fig. 6.

5. Discussion

In the preceding section, microtremors were found to have a wave nature approximately similar to the propagation of surface waves by means of examing the dispersion of phase velocities. Therefore, in order to explain the spatial variations of the amplitude of microtremors, the evaluation of the transmission and reflection coefficient of surface waves at a vertical discontinuity is attempted in this section.

An approximate method was devised to calculate the transmission and reflection of Rayleigh waves on a vertical boundary between two welded quarterspaces (Chen and Alsop, 1978[8]; Alsop, Goodman and Gregersen, 1974[6]). They consider the Rayleigh waves as resulting from a superposition of propagating homogeneous plane P and SV waves in a surface layer and an inhomogeneous plane P and SV waves falling off with depth in the half-space. This method is based on satisfying all boundary conditions on the vertical interface and computing the coupling between

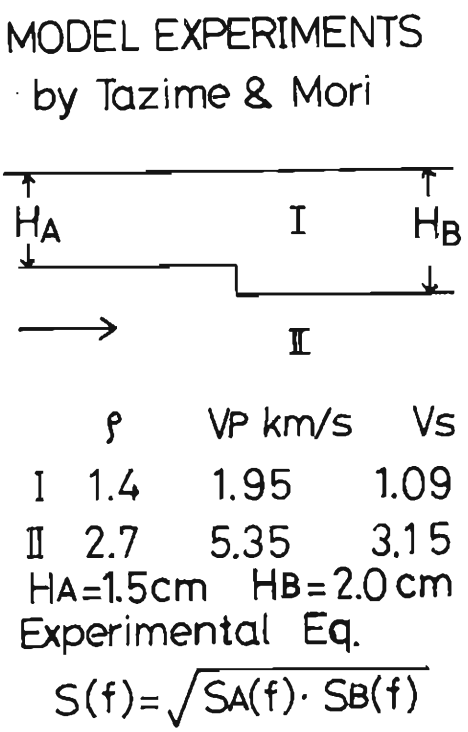

Fig. 9. Model used in the experiment by Mori and Tazime[9].

the interface stress-displacement pattern and the transmitted/reflected Rayleigh modes. This method of computation is introduced in the above two papers.

Model experiments are the most favorable way to confirm the accuracy of the theoretical values approximately computed in the above method. Mori and Tazime (1968)[9] performed model experiments for Rayleigh waves in layered elastic media having a step as shown in Fig. 9. This model is very similar to a schematic model of the underground profile in our study area. They obtained the following empirical formula.

When Y1 and Y2 are the spectra obtained at a distance, $\triangle$, for the thin and the thick-layer model flatly stratified, the spectrum Y, which is observed at the layer model with a step, is always almost equal to $(Y1 \cdot Y2)^{1/2}$. Y1, Y2, $(Y1 \cdot Y2)^{1/2}$ and Y are shown by Fig. 10,

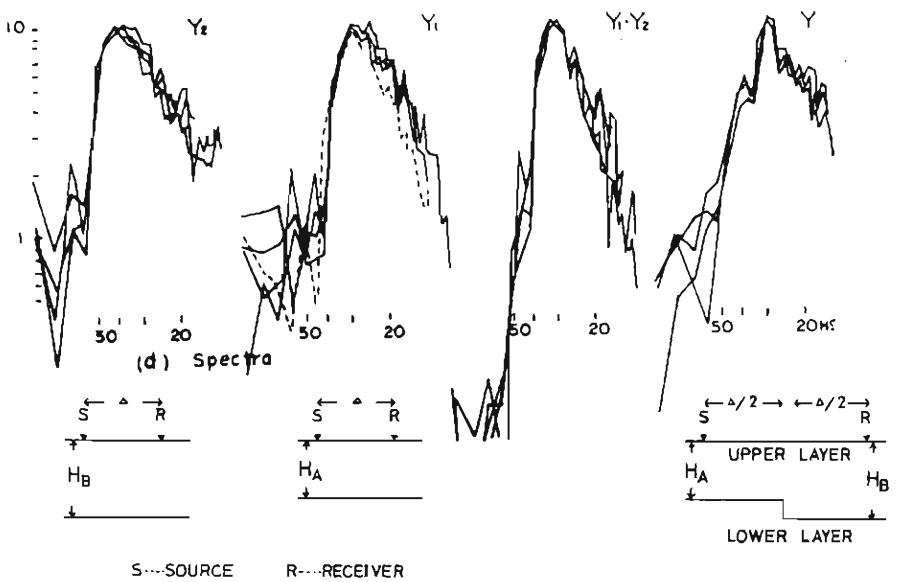

Fig. 10. Observed spectra for the model shown in Fig. 9 (after Mori and Tazime, 1968)[9].

which were obtained by their experiments. The empirical formula for the transmission coefficient at the discontinuity is expressed as $(Y1 \cdot Y2)^{1/2}/Y1$, when the surface waves propagate from the thin to the thick-layer side.

A comparison is made in Fig. 11 between the transmission coefficients computed by Alsop's method and those estimated by the above empirical formula. Instead of the observed spectra Y1 and Y2, the spectra $S_A(f)$ and $S_B(f)$ are used in this paper, which are theoretically obtained by means of Harkrider's formulation (Harkrider, 1964)[10] for excitation functions of Rayleigh waves in flat multi-layered media. Thus, the transmission coefficients at the discontinuity are estimated semi-empirically to be $\sqrt{S_A(f) \cdot S_B(f)}/S_A(f)$, in propagation from side A to side B. In Fig. 11, T_{AB} and S/S_A show the theoreti al transmission coefficients by Alsop's method and the semi-empirical ones for

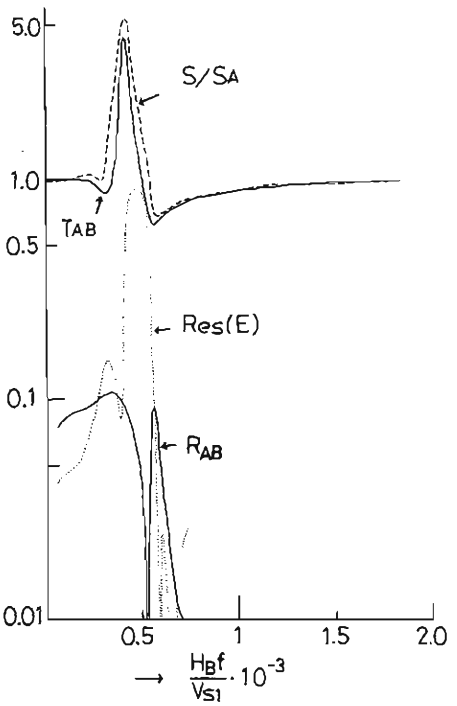

Fig. 11. Comparison of the transmission coefficients calculated by Alsop's method with those estimated by semi-empirical formula based on the model experiments by Mori and Tazime. The Model is shown in Fig. 9.

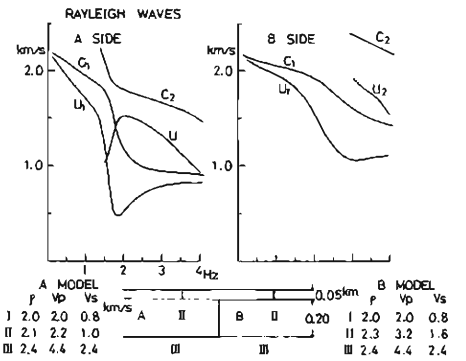

Fig. 12. Phase and group velocities of Rayleigh waves, assumed to be flat layers. C_1, C_2; phase velocities of the fundamental and the first higher mode. U_1, U_2; group velocities of the fundamental and the first higher mode.

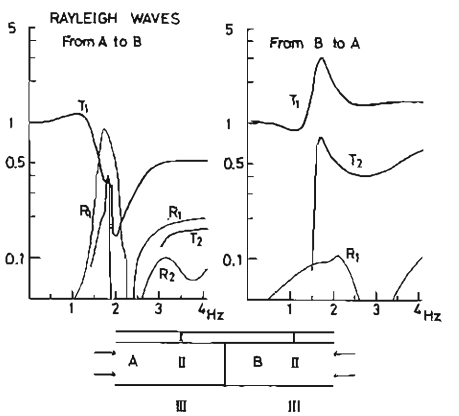

Fig. 13. Transmission and reflection coefficients of Rayleigh waves for propagation from thick to thin layer side (left) and from thin to thick layer side (right). T_1 and R_1 are trensmission and reflection coefficients for the fundamental mode.

the experimental model by Mori and Tazime shown in Fig. 9. The theoretical values T_{AB} agree well with the semi-empirical ones S/S_A in the peak frequency and the spectral shape, though their absolute values are somewhat different. The theoretical reflection coefficients cannot be compared with the experimental ones. It is reported that the reflection coefficients obtained by experiments, as noted here, are too small to be measured accurately (Mcgarr and Alsop, 1967)[11]. Res (E) in Fig. 11 shows residual energy. It is expressed as the differences of energy flows between two welded quarter space, being a criterion for accuracy of computation. Although the errors of the computation increase considerably around the peak frequency, the approximate method by Alsop, et al. may be satisfactorily valid to interprete the spatial variations of the amplitude characteristics of microtremors.

The cross section of the underground structure in this study area is simplified as shown in the lower portion of Fig. 12. P and S wave velocity and thickness of the layers are inferred based on the exploration data noted in the previous section. Model A and B correspond to the underground model of side A and B, respectively, as shown in Fig. 7. Phase and group velocities are shown in the upper portion of Fig. 12, which are computed from an assumption of flat layers. The frequency of the minimum group velocity of the fundamental mode for model A seems to be in favorable agreement with the predominent frequency of the power spectra of the vertical components on side A, but that for model B is in disagreement with the predominant frequency on side B.

The transmission and reflection coefficients for the propagation from A to B, i.e. the thick-layer side to the thin-layer one are shown in the left of Fig. 13, and those for the opposite propagation direction in the right. The transmission coefficients, T_1, from side A to B are either nearly unity or less than unity in any frequency range, depressing especially steeply in the range from 1.5 to 2.5 Hz and having a trough around 2 Hz. The reflection coefficients, R_1, in this propagation direction increase steeply in the narrow band around 1.75 Hz. On the other hand, the transmission coefficients from side B to A are either nearly unity or larger than unity in any range, having a peak around 1.75 Hz, and the reflection coefficients are very small in any ranges. The Rayleigh waves are found to give rise to an abrupt decrease in the frequency range from 1.5 to 2.5 Hz when propagaing from a thick-layer side to a thin-layer one and an abrupt increase in the same range when propagating from a thin-layer side to a thick-layer one.

The spatial variations of the amplitude characteristics of microtremors in this area are arranged in Fig. 14. The middle figures show the spectral ratios between the two points, which may be across the postulated fault. The ratio taken, is (the east side point)/(the west side point). The left and the right figures show the ratios between the two points on the west of the fault and on the east, respectively. The observed results of the spatial variations of microtremors are in agreement with the transmission characteristics theoretically computed in the propagation of Rayleigh waves from thick to thin-layer side (see the mid-bottom of Fig. 14). This is con-

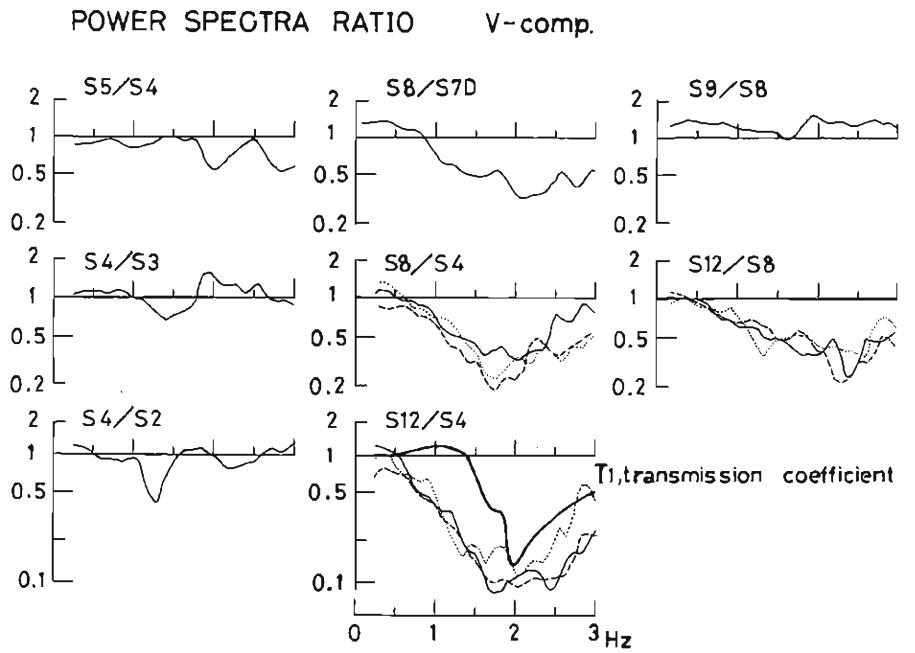

Fig. 14. Ratios of square roots of power spectra between the two point. The middle figures show the ratios between two points which may be across the postulated fault. The left and the right figures show the ratios between two point on the west of the fault and those between two points on the west, respectively.

sistent with the fact that most noise sources such as roads and streets are distributed westward.

Similar discussions can be made for the horizontal components of microtremors. It has already been discussed in section 3 that the power spectral ratios of the horizontal components between the two points across the fault have lower peak frequencies than those of the vertical ones, as shown in Fig. 3a, 3b and 3c. This suggests that the horizontal components should be considered to be different wave-types from the vertical components, probably Love waves.

It is difficult in this area to determine the phase velocities of the horizontal components from the phase differences between the two points because the horizontal components are contaminated by some different kinds of wave-types, such as SH-typed waves and SV-typed ones. Hence, detailed discussions of the natures of the horizontal components can not be made sufficiently. The comparison was already made in another paper (Irikura and Kawanaka, 1978)[12] between the theoretical transmission/reflection-coefficients at the discontinuity for Love waves and the power-spectra ratios observed. Phase and group velocities are shown in Fig. 15, computed from an assumption of flat layers without the vertical discontinuity. The computations are made for two cases of one layer model, each having a different

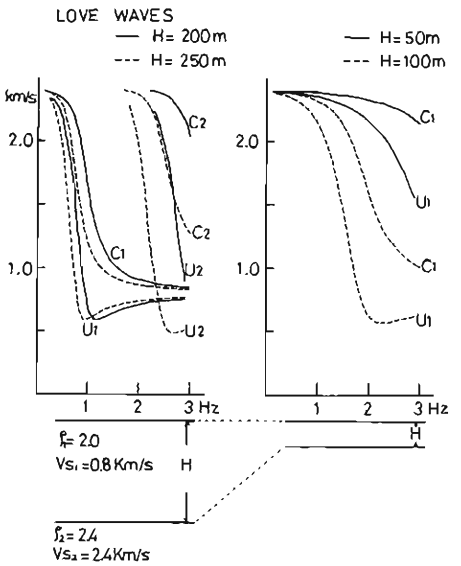

Fig. 15. Phase and group velocities fo Love waves, assuming to be flat layers.

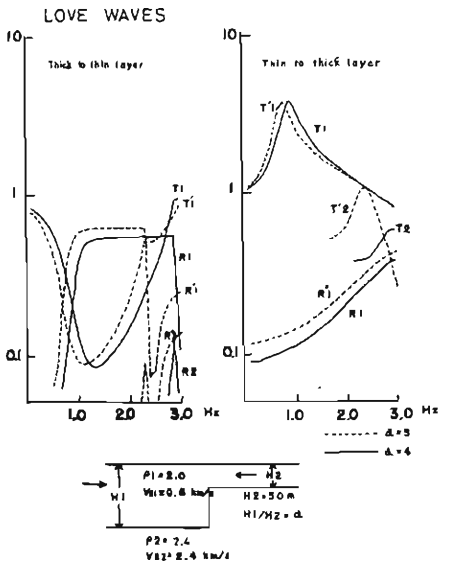

Fig. 16. Transmission and reflection coefficients for propagation from thick to thin layer (left) and from thin to thick layer. T, R; transmission and reflection coefficients in the model of $H_1/H_2=4$. T', R'; Those in the mosel of $H_1/H_2=5$. Subscript numbers mean mode numbers.

thickness of soil layer, and which are more simplified than the case of Rayleigh waves. The transmission and reflection coefficients of Love waves at the vertical discontinuity are shown in Fig. 16. The transmission coefficients have a trough around 1.3 Hz for propagation from the thick to the thin-layer side and a peak around the same frequency for the opposite propagation in the model of H1/H2=4.

The power spectral ratios of the horizontal NS and EW components, S4/S12 and S4/S8 shown in Fig. 3b and 3c, are examples of the spatial variation of the power spectra observed at two points across the Obaku fault. Those have a significant common-peak arround 1.2 Hz. These observed results may be considered to be in good agreement with the transmission characteristics in propagation from the thick to the thin-layer side theoretically computed for the model of H1/H2=4. The peak frequency of the transmission characteristics shows a significant variation with the ratio of the thickness of the thin layer to that of the thick one, H1/H2. Then, we can determine the appropriate value, H1/H2, so that the theoretical transmission characteristics coincide with the observed results of the spatial variations of microtremors.

The models of the ground layers for Rayleigh and Love waves are somewhat different, although the theoretically calculated values coincide fairly well with the

observed results in the both cases. We cannot determine which models are better using only the present data. However, in this study the model for Rayleigh waves is considered to be more realistic, because the model for Love waves are over-simplified owing to lack of phase velocities determined by the observed horizontal components.

6. Conclusion

The spatial variations of the power spectra of microtremors are found to be related to horizontal irregularities of underground structures. The amplitudes at the sites underlain by thick soil-deposits are remarkably larger than those at the sites underlain by thin ones, even if those sites are adjacent to each other. However, a correlation between the predominant frequencies and the thickness of the soil deposits does not always exist. The power-spectral ratios between the two points show a remarkable variation, depending on whether vertical discontinuities exist between those points or not.

In this area near the eastern edge of the basin, microtremors seem to propagate from the plain side to the hill side. This corresponds to the propagation from the thick to the thin-layer side. The phase velocities of vertical components at the thick-layer side show dispersive nature of Rayleigh waves. On the other hand, those at the thin-layer side show dispersive nature in the higher-frequency range in which the wave lengths are shorter than the layer-thickness at the thin layer side, but remain the old modes of the thick layer side for a short while in the lower frequency range in which the wave-lengths are longer than the thickness of the thin layer.

The observed results of the spatial variations of the characteristics of microtremors are found to be explained in terms of the transmission/reflection of surface waves at the vertical discontinuity. The vertical components are clearly considered to be Rayleigh waves and the horizontal ones may be regarded as Love waves with less confidence.

The microtremor data are very useful as one of basic sources of information for seismic microzoning, if the power spectra and the phase velocities are obtained spatially.

Acknowledgements

The authors wish to express their sincere thanks to Prof. Soji Yoshikawa for his encouragement, and also to Associate Prof. Yoshimasa Kobayashi of Kyoto University for his helpful advice in carrying out this work. The authors are especially grateful to Mr. Masao Nishi for his co-operation in the observation.

The data processing was run on a FACOM 230-25 at the Information Data Processing Center for Disaster Prevention Research, of Disaster Prevention Research Institute of Kyoto University and the numerical computations were run on a FACOM M-200 at Data Processing Center of Kyoto University.

References

1) Poceski A.: The Ground Effect of the Scopie July 26 1963 Earthquake, Bull. Seism. Soc. Am., Vol. 59, 1969, pp. 1–22.
2) Murai, I., N. Tsunoda and Y. Tsujimura: Inquiry Survey of Intensity Distributions on the Northern-Yamanashi earthquake in 1976, Proc. 14th Japan Natio. Cong. Natur. Disast. Sci., 1977, pp. 387–388 (in Japanese).
3) Sasaki, Y., Y. Fujino and M. Hakuno: Effects of Topographical Features on Earthquake-Induced Damage, Bull. Earthq. Res. Inst., Vol. 53, 1978, pp. 447–459 (in Japanese).
4) Kitsunezaki, C., N. Goto and Y. T. Iwasaki: Underground Structure of the Southern Part of the Kyoto Basin Obtained from Seismic Exploration and Some Related Problems of Earthquake Engineering, Annuals Disast. Prev. Res. Inst., Vol. 14A, 1971, pp. 203–207 (in Japanese).
5) Kobayashi, Y., K. Irikura, M. Masanori, F. Amaike, K. Kishimoto and S. Kasuga: Seismic Exploration of the Obaku Fault, Annuals Disast. Prev. Res. Inst., Vol. 23 B–1, 1980, pp. 95–106 (in Japanese).
6) Alsop, L. E., A. S. Goodman and S. Gregersen: Reflection and Transmission of Inhomogeneous Waves with Particular Application to Rayleigh Waves, Bull. Seism. Soc. Am., Vol. 64, 1974, pp. 1935–1952.
7) Kanai, K., T. Tanaka and S. Yoshizawa: On Microtremors. IX. (Multiple Reflection Problem), Bull. Earthq. Res. Inst., Vol. 43, 1965, pp. 577–588.
8) Chen, T. C. and L. E. Alsop: Reflection and Transmission of Obliquely Incident Rayleigh Waves at a Vertical Discontinuity, Bull. Seism. Soc., Am., Vol. 69, 1979, pp. 1409–1424.
9) Mori and Tazime: Some Considerations on the Results from Short Period Surface Wave Dispersion, Geophy. Bull. Hokkaido University, Vol. 19, 1968, pp. 81–91 (in Japanese).
10) Harkrider, D. G.: Surface Waves in Multilayered Elastic Media I. Rayleigh and Love Waves from Buried Sources in a Multilayered Elastic Half Space, Bull. Seism. Soc. Am., Vol. 54, 1964, pp. 627–679.
11) McGarr, A. and L. E. Alsop: Transmission and Reflection of Rayleigh Waves at Vertical Boundaries, J. Geophys. Res., Vol. 72, pp. 2169–2180.
12) Irikura, K. and T. Kawanaka: Characteristics of Microtremors in a Ground with Steeply Varying Structure, Proc. 5th Japan Earthq. Engin. Symp., 1978, pp. 297–304.